arXiv:0910.3599v1 [cond-mat.supr-con] 19 Oct 2009

Electronic Structure, Localization and Spin-State Transition in Cu-substituted FeSe: $Fe_{1-x}Cu_xSe$

Stanislav Chadov,* Daniel Schärf, Gerhard H. Fecher, and Claudia Felser
Institut für Anorganische Chemie und Analytische Chemie,
Johannes Gutenberg - Universtität, 55099 Mainz, Germany

Lijun Zhang and David J. Singh
Materials Science and Technology Division, Oak Ridge National Laboratory, Oak Ridge, TN 37831-6114, USA

(Dated: October 19, 2009)

We report density functional studies of the $Fe_{1-x}Cu_xSe$ alloy done using supercell and coherent potential approximation methods. Magnetic behavior was investigated using the disordered local moment approach. We find that Cu occurs in a nominal d^{10} configuration and is highly disruptive to the electronic structure of the Fe sheets. This would be consistent with a metal insulator transition due to Anderson localization. We further find a strong cross over from a weak moment itinerant system to a local moment magnet at $x \approx 0.12$. We associate this with the experimentally observed jump near this concentration. Our results are consistent with the characterization of this concentration dependent jump as a transition to a spin-glass.

PACS numbers: 74.25.Jb,74.25.Ha,74.62.Dh
Keywords: DLM, CPA, FeSe, superconductivity, spin glass

I. INTRODUCTION

The discovery of high-temperature superconductivity in Fe compounds[1] has led to widespread interest both in understanding the superconductivity and in unraveling the normal state properties of these unusual materials. These Fe-based materials and cuprates are the only known superconductors with critical temperatures exceeding 50 K. Therefore it is natural that the relationship between these two classes of materials has been the focus of much investigation. At present, it seems that the Fe-based materials are rather different from cuprates at least from an electronic point of view – in particular they do not show Mott insulating phases, and generally appear to manifest more metallic, itinerant electron physics than cuprates.[2,3,4] It is unclear whether this means that the Fe-superconductors are fundamentally different from the cuprates, or whether there is a more subtle connection that remains to be found.

In this regard, the FeSe binary provides a particularly useful material for investigation both because of its relative simplicity and because of the rich variety of properties including superconductivity[5,6] found in it, as well as in the related FeS, FeTe and alloy systems. FeSe represents a robust superconductor with a remarkable increase of T_C under pressure reported by many groups.[5,6,7,8,9,10] Furthermore, this system is chemically amenable to a wide variety of substitutions while still admitting the growth of high quality crystalline samples. The response of metallic materials to disorder and scattering of various types (magnetic, non-magnetic, etc.) induced by substitutions is a potentially very useful probe of the robustness of the metallic phase and of the relationship of physical properties and itinerant electron physics.

The fact that the Fe-based superconductors are less strongly correlated than cuprates more readily allows the use of standard electronic structure methodology to make connections with experiment. However, we note that there remain significant errors in the density functional description of these materials, *e.g.* in the interplay between structure and magnetism, likely due to strong spin fluctuations.[11,12] In any case, similar to the other Fe-based superconductors[13,14,15,16], first principles investigations of Fe chalcogenides[17] imply very similar physics for the pnictide and chalcogenide superconductors.

Stoichiometry is an important issue for FeSe. The material typically forms with some amount of excess Fe, which occupies a crystallographic site outside the Fe plane. The formula may therefore be written as $Fe_{1+x}Se$ or equivalently $FeSe_{1-y}$. Here we use the former notation to emphasize the additional Fe site. There have been attempts to modulate the excess Fe by alloying with Co (by substitution) or Na (by intercalation).[18] According to that work, the number of excess valence electrons (i.e. the experimental doping level of the samples) was $x \approx 0.027$ for Co and $x \approx 0.03$ for Na. In both cases the T_C was approximately 8.3 K. Other experiments[10] showed that $x = 0.01$ is already sufficient to keep the superconductivity. At the same time the upper value of x is bound by oxygen contamination.[19] In another work[20] the same authors reported that the strongest superconducting signal is observed closer to stoichiometry ($x = 0.01$) and that at $x = 0.01$ the system is much closer to the ideal tetragonal phase, while less stoichiometric samples have a weaker superconducting transition and magnetic contamination. The fact that with $x \to 0$ the system has stronger superconductivity and at the same time becomes magnetically and structurally unstable are indications that there may be a quantum critical point (QCP) nearby. This view is supported by the fact that near ideal stoichiometry $Fe_{1.01}Se$ shows a tetragonal to orthorhombic distortion as it is cooled through 90K.[21] In other Fe-based superconductors this type of distortion occurs as a precursor to the spin density wave (SDW) magnetic ordering (or coincident with the SDW), but $Fe_{1.01}Se$ does not show SDW ordering down to the lowest temperature.

In fact, many authors have discussed the association between magnetism and superconductivity in these materials, with superconductivity appearing when magnetism is suppressed.[22,23,24] While there is much work pointing at the possibility of a QCP affecting the physics of the Fe-based superconductors, there is not yet an established consensus regarding its nature. On the one hand it has been argued that there is a nearness to localization driven by Coulomb interactions and that this underlies a quantum critical point.[25] However, the phase diagrams do not show Mott insulators, and in fact the magnetic phases, including the spin-density wave (SDW) phase are unambiguously metallic,[2] suggesting a quantum critical point associated with itinerant magnetism. Experiments probing the details of the interplay between magnetic order and superconductivity are complicated by the fact that chemical disorder in doped samples makes investigation of the critical point difficult. As we discuss here, results for FeSe indicate that it is very close to the magnetic quantum critical point and therefore may be a very useful system for elucidating the associated physics.

Before proceeding we mention previous first principles studies of defects and doping in iron chalcogenides. Regarding excess Fe, Lee and co-workers early on showed that chalcogen vacancies if present will lead to the formation of ferrimagnetic clusters in FeSe and FeTe,[26] while Zhang and co-workers found that excess Fe in the $Fe_{1+x}Te$ system serves both as an electron dopant and also a magnetic impurity. Han and Savrasov[27] reported a detailed analysis of the magnetic instabilities and magnetic ordering in relation to the Fermi surface as a function of excess Fe concentration.

The present work is motivated by recent experimental findings for Cu-substituted $Fe_{1.01}Se$.[28] In particular, it was found that Cu substitutes for Fe in the Fe plane, and that there is a rapid suppression of T_C in the concentration range $0-4\,\%$ and a subsequent metal–insulator transition at $\sim 4\,\%$. Furthermore, there is a development of dynamical magnetic fluctuations detected by NMR, which noticeably rise at $\sim 12\,\%$ of Cu substitution. We begin with supercell calculations addressing the chemistry and local electronic structure, and then proceed to investigate the electronic structure in more detail using coherent potential approximation (CPA) calculations for the disordered alloy.

II. SUPERCELL CALCULATIONS

First principles calculations were performed using 2x2x1 and $2\sqrt{2}$x$2\sqrt{2}$x1 supercells based on tetragonal FeSe (see Fig. 1) with one Fe replaced by Cu. This corresponds to Cu concentrations, x in $Fe_{1-x}Cu_xSe$ of x=0.125 and x=0.0625, respectively. These calculations were done using the generalized gradient approximation of Perdew, Burke and Ernzerhof (PBE).[29] The lattice parameters of the supercells were fixed to the experimental values for x=0.12 and x=0.06 as reported in Ref. 28. However, the atomic positions within the cell were determined by energy minimization. This structural relaxation was performed using the projector augmented wave (PAW) method as implemented in the VASP code,[30] with an energy cut-off of 350 eV. The relaxed structures showed some expansion of the lattice mainly in the in-plane direction around the Cu impurity sites. The relaxed Cu-Se bond lengths were $\sim$ 2.44 Å, as compared to Fe-Se bond lengths of 2.25Å-2.33Å. This is consistent with the increase in in-plane lattice parameter seen experimentally.[28,31] The electronic structures were calculated using the more precise general potential linearized augmented plane-wave (LAPW) method,[32] with the augmented plane wave plus local orbital (APW+LO) implementation[33] of the WIEN2k code.[34] LAPW sphere radii of 2.1 a_0 for all sites, with well converged basis sets and zone samplings were used in this calculation. The consistency of the PAW and LAPW calculations was checked via the LAPW forces for the structures obtained via total energy relaxation with the PAW method. The maximum force in the LAPW calculation was 2 mRy/a_0.

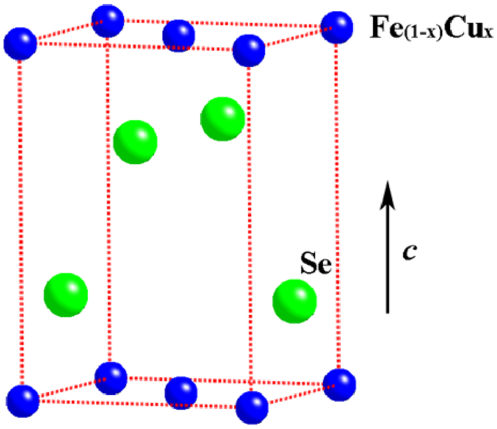

FIG. 1: (color online) Crystal structure of $Fe_{1-x}Cu_xSe$.

The electronic density of states for the two supercells is shown in Fig. 2, while the average Fe and Cu d contributions as defined by projections onto the LAPW spheres are shown in Fig. 3. As may be seen the Cu d bands are at $\sim$ 3 eV binding energy, and are therefore fully occupied for a nominal d^{10} Cu configuration. We also note that there are shifts in the Fe density of states as seen in Fig. 2. These shifts are consistent with electron doping. However, substitution of a nominal Fe^{2+} by Cu^{1+} would ordinarily be expected to lead to hole and not electron doping. This suggests a bonding rearrangement involving Se around the Cu site. There is also some Cu d contribution to the bands above the Fermi level E_F indicating covalency involving Cu d states. However, the magnitude (see Fig. 3) seems inadequate to explain the observed electron doping, implying that Se-Se bonding

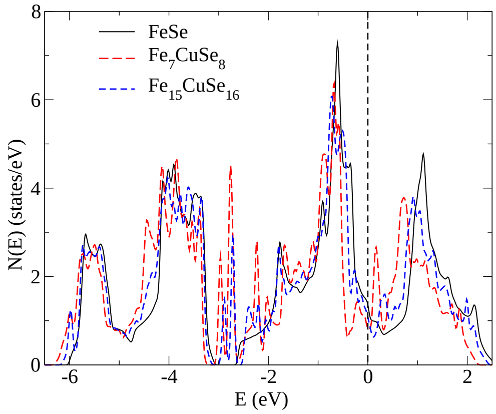

FIG. 2: (color online) Total electronic density of states for $Fe_{1-x}Cu_xSe$ supercells on a per formula unit basis. The Fermi energy is at 0 eV.

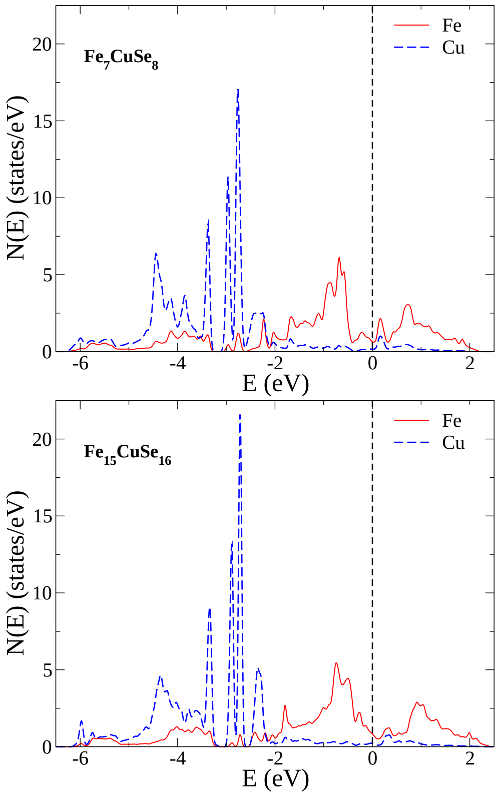

FIG. 3: (color online) Fe and Cu d contributions to the density of states for the x=0.125 (top) and x=0.0625 (bottom) supercells. These are given by projections onto the LAPW spheres for Cu and averaged over the Fe sites, on a per atom basis.

may be important around the Cu site. This is similar to findings for CuSe in various structural modifications showing an interplay of different bonding types.[35]

In any case, from the positions of the Cu d states at high binding energy it is clear that Cu substitution is highly disruptive to the electronic structure of the Fe sheets in FeSe. This is in contrast to the case of Co in the arsenides, which leads to the formation of a coherent electronic structure with effective doping.[36] As such, Cu alloying cannot be considered with the virtual crystal approximation, and more sophisticated treatments such as the coherent potential approximation (CPA)[37,38,39] are needed. Considering the strong scattering implied by this result, localization could be caused by disorder, i.e. Anderson localization,[40] should be considered in the context of the insulating phase that develops at Cu concentrations above 4%. Finally, in view of the proximity of these phases to magnetism, disruption of the electronic structure by scattering (which works against itinerancy) would be expected to lead to the formation of local moments around the Cu sites. These would be distributed over the Fe atoms around the Cu, but because of the d^{10} configuration would not exist on the Cu atoms themselves.[41]

III. COHERENT POTENTIAL APPROXIMATION CALCULATIONS

Our CPA calculations were performed using the tetragonal structure (Space group: 115) (see Fig. 1), with lattice parameters from experiment,[28] similar to the supercell calculations described above. Additionally, in these calculations we used experimental atomic positions. It follows that with Cu substitution the system linearly expands in the plane containing Fe atoms and linearly shrinks in the perpendicular direction. The volume increases weakly with Cu content. At the same time, the position of the Se atoms (not fixed by the point group symmetry), remains practically constant and is here set to z = 0.2707 (in multiples of the c lattice parameter). Interestingly, by extrapolating the lattice parameters up to 50 % Cu one arrives very close to the structure of one of the modifications of $CuFeSe_2$.[42] That material is a semiconductor with low-temperature magnetism.[42,43]

The idea of the CPA is to replace the random array of real on-site potentials by an ordered array of effective potentials. The scattering properties of the effective potential are than determined self-consistently in terms of the local mean-field theory with the condition that the total Green's function of the effective system does not change upon replacement of the single effective potential with the real one. This idea is sketched in Fig. 4.

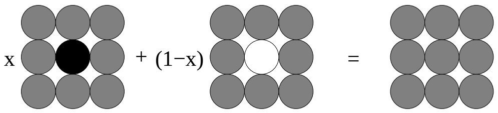

FIG. 4: The CPA model: the Green's function of the effective medium (gray atoms) is obtained as an average of the partial impurities Green's functions (black and white atoms).

The computational cost of CPA calculations is significantly lower than supercell approaches where the disorder is approximated by a randomly generated configurations within a large number of large supercells. The important advantage is that the CPA does not affect the translational (as well as the point group) symmetry of the unit cell whereas the supercells must be chosen sufficiently large to avoid effects from the assumed order or periodic images, which are caused by an artificial translational symmetry. The CPA allows investigation of the electronic structure as a continuous function of the substitution level, which is very important describing phase transitions as well as in studying the evolution of the electron structure with concentration. The CPA also provides type-resolved contributions of the different local quantities. The disadvantage is that as any mean-field theory, the standard CPA does not include the local environment effects such as preferential ordering,[44] the Invar effect[45,46] and lattice relaxations around the impurity site. The low concentrations of interest here, and the results of the supercell calculations, which find modest changes in local structure, indicate that the effects of local ordering and lattice distortion are not likely to be the crucial factors in determining the electronic structure of the alloy.

The $\mathrm{Fe}_{1-x}\mathrm{Cu}_x\mathrm{Se}$ system is known to be non-magnetic, in the sense of not having ordered magnetism, over the investigated range of Cu concentrations. However, as mentioned, there is experimental evidence that magnetic fluctuations noticeably strengthen above 12 % Cu. The consistent way of studying these fluctuations is to determine the coefficients A_i of the Ginzburg-Landau energy expansion $E = E_{\mathrm{PM}} + \sum_i A_i M^{2i}$ in the local magnetization M.[47] The best local approximation to the disordered paramagnetic state E_{PM} is given by the so-called *disordered local moments* (DLM) approach,[48,49] which is used in the present work. The DLM effective medium gives an accurate representation of a paramagnetic state with randomly oriented spins by using an equiatomic random alloy of spin-up and spin-down atoms, in complete analogy to the CPA (see Fig. 5).

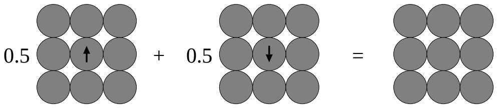

FIG. 5: The DLM model: the Green's function of the effective non-magnetic medium is obtained as an average of the partial polarized impurity Green's functions.

In this context the DLM picture provides a common basis to study different types of possible magnetic order. The important feature of the DLM is the consistent description of the paramagnetic state for the systems with itinerant and local moment behavior;[47,50] local moment systems keep their finite moments in the paramagnetic state whereas itinerant systems become locally non-magnetic. The essential assumption of the DLM is the quasi-static treatment of fluctuations. It assumes that the fluctuations of the local magnetic moment are much slower than the electron motion, so that the instantaneous band structure corresponds to the equilibrium electronic state. This should lead to a certain overestimation in case of large fluctuating magnetic moments and to a certain suppression in case of small moments, by sharply emphasizing magnetic transitions.

Here we use the KKR (Korringa-Kohn-Rostoker) method in the Munich SPR-KKR (spin-polarized relativistic) package[51] for our CPA calculations. These calculations were done with the local spin-density approximation (LSDA) in the form of Vosko, Wilk and Nusair[52]. Here we use the full-symmetry potential (FP) method to account for the non-spherical contributions to the one-electron potential. This is important because the layered structure of FeSe is strongly anisotropic. As expected, relativistic effects are found to be relatively small. Thus although the calculations are fully relativistic, only spin moment is reported in the following as the orbital moments are found to be negligibly small.

The effective DLM medium is represented by the random $\mathrm{Fe}_{0.5}\mathrm{Fe}_{0.5}$ alloy, with $\pm\, 2\,\mu_{\mathrm{B}}$ anti-parallel spins initially induced for each on-site component. The system is then allowed to relax during the self-consistent iteration process. In case of locally non-magnetic solutions the proximity of the system to the magnetic state is estimated by considering the Fe local spin susceptibility $\chi = d\mu/dB_{\mathrm{ext}}|_{\mu=0}$. This is calculated by applying the small external local magnetic field of $dB_{\mathrm{ext}} = 2$ mRy.

The symmetry of the magnetic fluctuations are considered to be characterized by the exchange coupling constants J_{ij} of the Heisenberg local moments picture: $H_{\mathrm{eff}} = -\sum_{i>j} J_{ij}\vec{\mu}_i\vec{\mu}_j$, where $\vec{\mu}_i$ is the local magnetic moment of the i-th atomic site. However, it should be emphasized that the use of a Heisenberg model in analyzing low energy magnetic fluctuations does not necessarily imply local moment magnetism. Here, the so-called real-space formalism is utilized[53]. Again, in case of the non-magnetic solution, a magnetic moment is induced by a small external field of 2 mRy.

IV. CPA RESULTS

Magnetic moments and susceptibility

Regardless of the calculation mode (magnetic or non-magnetic, fully- or non-relativistic, spherical or non-spherical potential), we find that all properties (density of states (DOS) at the Fermi energy, magnetic moments, susceptibility, etc.) calculated as a function of x exhibit discontinuities or jumps at a Cu concentration, $x_{\mathrm{m}} \approx 12\%$. Importantly, this concentration corresponds remarkably well to the experimentally observed onset of the dynamical magnetic fluctuations.[28] The DLM calculations lead to the appearance of local moments at the Fe site that vary weakly within a given regime: low Cu-concentration ($x < x_{\mathrm{m}}$) or high Cu-concentration ($x > x_{\mathrm{m}}$) (Fig. 6(a)).

Within the low Cu-concentration regime the magnetic moment is suppressed almost to zero ($\sim 10^{-3}\,\mu_{\mathrm{B}}$), how-

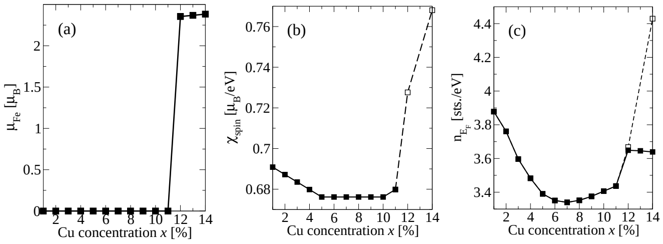

FIG. 6: Local magnetic moments of Fe (a), local spin susceptibility (b) and the total DOS at the Fermi energy (c) calculated as a function of Cu concentration. Filled squares mark DLM, hollow squares - non-magnetic calculations.

ever at $x = x_m$ it rises sharply to about 2.35 μ_B. The Fe local spin susceptibility shows a similar discontinuous behavior at $x = x_m$, as shown in Fig. 6(b). On the other hand, besides the sharp magnetic transition at x_m, the magnetic susceptibility indicates that the system approaches magnetism in the low Cu-concentration regime as well, however its ground-state remains non-magnetic. As may be seen (Fig. 6(c)), the changes in magnetic behavior as a function of x closely follow the behavior of the density of states at the Fermi energy and is therefore related to the band structure.

We emphasize that the DLM calculations provide information about moment formation in the disordered (paramagnetic) state, not directly about magnetic ordering. In fact, at the LSDA or GGA levels FeSe is already unstable against magnetic ordering, specifically against SDW order.[17] This ordering is presumably suppressed by spin-fluctuations the detailed nature of which is not fully understood at present, but which might be central in understanding the superconductivity of these phases. What a cross-over from a non-magnetic to a state with moments in the DLM indicates is a cross-over from a state that may have itinerant magnetism to a state with stable moments independent of ordering. This is therefore a change in the nature of the magnetism at this value of x. While such a cross-over is not directly a QCP it may be an indicator. FeSe, as mentioned, does not show long range magnetic order, but magnetic ordering is very difficult to avoid in clean metals with stable moments and electronic structures that are neither low-dimensional nor geometrically frustrated. The effect of the disorder induced by relatively low amounts of Cu alloying appears to be a change of magnetic character from a softer moment (itinerant) regime to a regime with more robust local moments.

Exchange coupling

Turning to the exchange couplings, we find very small inter-plane interactions below the precision of the calculations. Furthermore, the in-plane contributions are significant only for the first four in-plane coordination circles. The corresponding values are shown as a function of Cu concentration in Fig. 7.

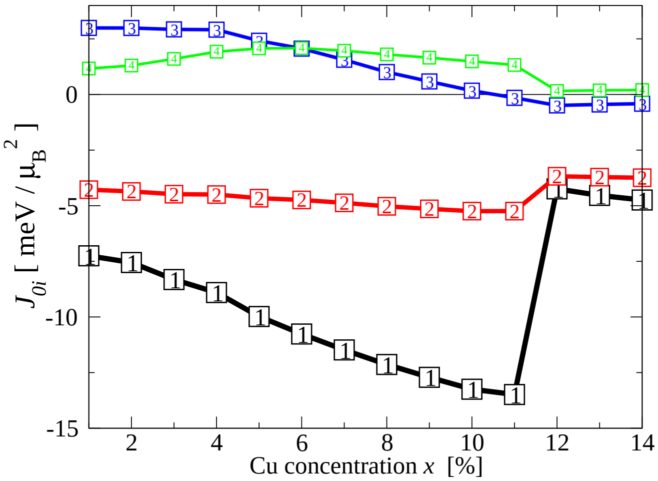

FIG. 7: (Color online) Exchange constants J_{oi} ($i = 1, 2, 3, 4$) for the 4 nearest-neighbor in-plane couplings as a function of Cu concentration. Each J_{0i} coupling curve is marked by corresponding index i.

Since in the range of $x < x_m$, J_{01} has larger amplitude than J_{02}, while the number of the first- and second-nearest neighbors is the same, the nearest antiferromagnetic order seems to be more preferable. For the pure FeSe the particular order was already studied in more details by other authors.[17,27,54,55] In the extrapolation from the low Cu-concentration limit the present exchange coupling constants agree well with those published before.[17,54] On the other hand, as we have seen, the system does not have stable magnetic moments within $x < x_m$.

The monotonously increasing amplitude of the nearest-neighbor coupling indicates the growing electron delocalization with increasing Cu content. However, at $x = x_m$ one observes a rapid suppression of all J_{ij}, which in turn indicates the sudden localization of the d-electrons and corresponds to the development of the strong atomic moments. In this regime $J_{01} \approx J_{02}$, while the higher-order coupling constants nearly vanish. This situation with stable local moments emerging at $x \approx 0.12$, competing exchange interactions, and disordered Cu positions (which correspond to sites with no moment) is consistent with the formation of a spin-glass.

V. BAND STRUCTURE ANALYSIS

Band structure

In the following we consider the Bloch spectral functions, which take the role of the band structure in the disordered system. These are plotted along the path shown in Fig. 8. The calculated DOS and the corresponding spectral functions are shown in Fig. 9. The general trend in the low Cu-concentration regime is the redistribution of the spectral weight from the M-A onto the Z-Γ line, by shifting the whole picture down in energy with respect to the Fermi level. Qualitatively, this is exactly what was found in our supercell calculations where in spite of the Cu d^{10} configuration, Cu substitution produces electron doping.

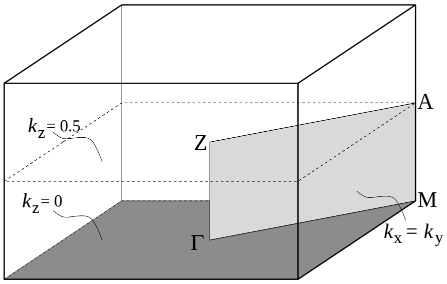

FIG. 8: The BZ scheme. The reciprocal (k_x, k_y, k_z)-coordinates are given in units of $(2\pi/a, 2\pi/a, 2\pi/c)$. The marked details are discussed in the text.

As in the other Fe-based superconductors the nearness to magnetism of FeSe is related to the electronic structure specifically the high density of states derived from Fe d orbitals and the nested Fermi surface. The Fermi energy at x=0 occurs towards the bottom of a pseudogap in the DOS. As seen in the Bloch spectral functions there are two effects as Cu is alloyed into the material. First of all the Fermi energy is raised and secondly, as a consequence of the disorder, the DOS as a function of energy is smoothed, filling in the pseudogap. This explains the initial decrease, followed by an increase in the tendency towards moment formation. When the Cu concentration reaches $x_{\rm m}$ value there is a dramatic change in the spectral function. Since the system develops large local moments, the DLM spin disorder leads to a strong incoherence in the bands.

Fermi surface

To study the nesting effects we track the substitution-induced transformation of the Fermi surface in the BZ. In the following we will consider the Fermi surface cross-sections by horizontal (k_z = const) and vertical ($k_x = k_y$) planes.

In general, the electronic structures of the Fe-based superconductors show disconnected Fermi surfaces consisting of hole sections around the zone center (along Γ-Z) and two electron sections at the zone corner (along M-A direction). Our calculated Fermi surface cross-sections (Fig. 10) are in good agreement with this picture.

It turns out that the growing chemical disorder with increasing Cu-concentration destroys the Fermi surface, especially affecting the hole-pockets (centered at Γ-Z). Since the in-plane hole–electron nesting is the main mechanism for the superconductivity in FeSe and related compounds,[17] the superconducting signal must strongly attenuate. Indeed, the experimentally measured $T_{\rm C}$ falls down very fast and completely vanishes at $x \approx 4$ %.[28]

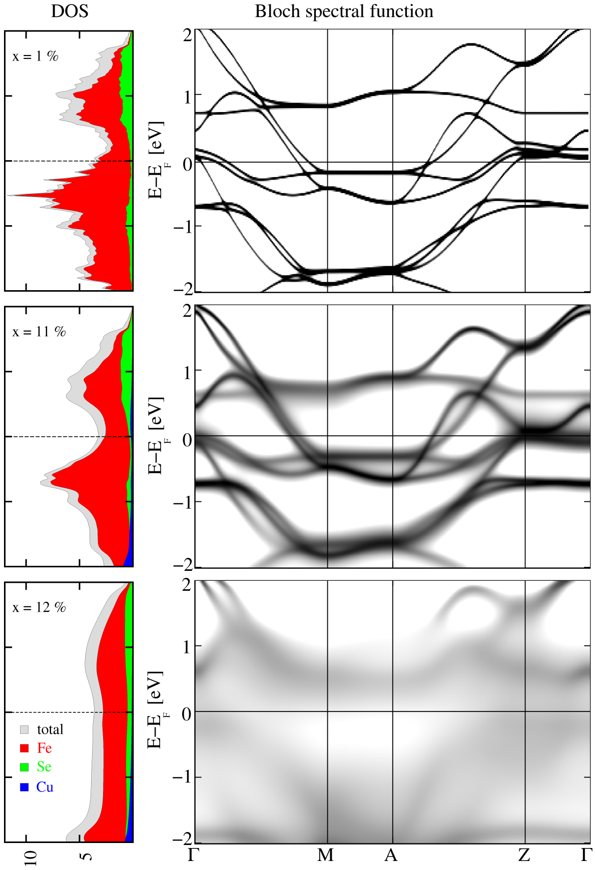

FIG. 9: (Color online) Atomic type-resolved DOS and the corresponding Bloch spectral functions for $x = 1, 11, 12\,\%$ as calculated within the DLM.

Although the reason for the magnetic transition can be understood in terms of the band structure (Fig. 9), it is still useful to observe the accompanying changes of the non-magnetic Fermi surface. The corresponding results for 11 % and forced non-magnetic calculations for 12 and 14 % are compared on Fig. 11. Here the low-weight contributions are cut off, otherwise the band structure analysis will be much complicated by chemical disorder.

Thus, the Fermi weight rapidly "spills" from $k_z = 0.5$ onto the $k_z = 0$ plane. This shows a loss of the Fermi surface in the $k_z = 0.5$ plane first as a function of Cu alloying although there is a strong loss of spectral weight at all k_z consistent with insulating character. At the same time the central figure does not blow up any more, but rather pulls the borders of the magnetic BZ (MBZ) (the two relevant in-plane MBZs are marked by the dashed and the dotted lines on Fig. 11). Analogous behavior was shown for the related $\rm Fe_{1+x}Te$ compound[27]: it was suggested that such redistribution of the Fermi weight between two neighboring MBZs reflects the competition between magnetic interactions of different symmetries. The inhomogeneity becomes especially sharp at $x = 14\,\%$, indicating that the system starts to prefer the certain in-plane magnetic order for $x > x_{\rm m}$.

Preferential accumulation of the Fermi weight on the

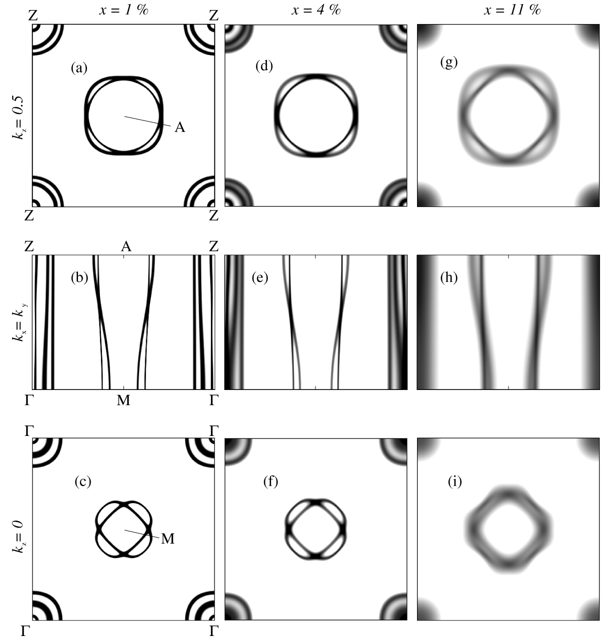

FIG. 10: Cross-sections of the Fermi surface in BZ by $k_z = 0.5$ (a, d, g), $k_x = k_y$ (b, e, h) and $k_z = 0$ (c, f, i) planes.

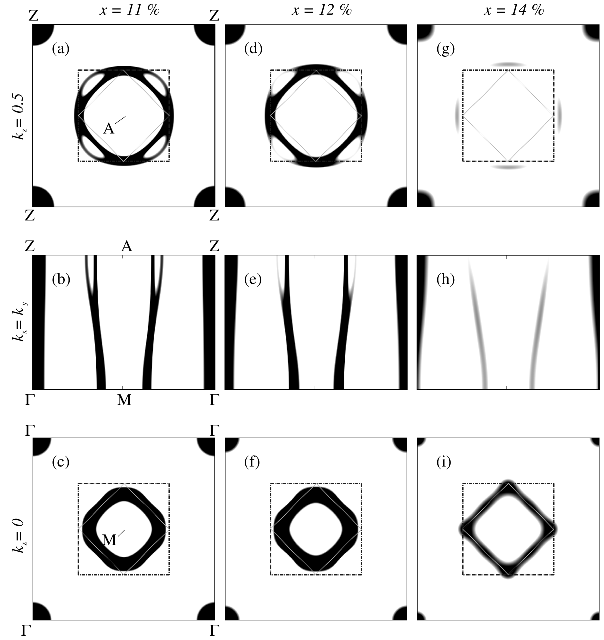

FIG. 11: Cross-sections of the Fermi surface in BZ by $k_z = 0.5$ (a, d, g), $k_x = k_y$ (b, e, h) and $k_z = 0$ (c, f, i) planes. Calculations are done within the non-magnetic regime.

edges of the corresponding MBZ in the $k_z = 0$ plane indicates the delocalization of the conduction electrons in real space. This delocalization becomes unfavorable, since the in-plane lattice spacing increases (the accompanying vertical real-space delocalization is a minor effect). At a certain point ($x = x_\mathrm{m}$) the system undergoes the localization transition. As a result, the strong magnetic moment arises. This rapid localization is also reflected by the reduced amplitude of the exchange coupling constants for $x > x_\mathrm{m}$ as discussed above.

VI. SUMMARY AND CONCLUSIONS

To summarize, we find that Cu occurs in a d^{10} configuration when alloying into FeSe. Nonetheless it serves as an effective electron dopant. Importantly, it is also a source of strong scattering. The calculated changes in the Bloch spectral function with alloying show no signs of gapping near the Fermi level over the concentration range studies. This situation suggests that the insulating phase occurring above $\sim 4\%$ Cu may be an Anderson localized system arising from disorder rather than a conventional semiconductor. The magnetic instability observed at about $12\,\%$ Cu is characterized as a spin-state like transition, where a soft moment near magnetic state at low x gives way to a state with stable disordered local moments at high x. This is consistent with the formation of a spin-glass especially considering the near compensation of nearest and next nearest exchange interactions. This is in accord with experimental observations[28].

The result that the Fermi weight for the electron sections at $k_z = 0.5$ is suppressed before that at $k = 0$ suggests a three dimensional character to the electronic structure and scattering above $x \sim 0.1$. It will be quite interesting to investigate this possibility experimentally, via single crystal transport or experiments under strain, especially uniaxial strain if this becomes feasible.

Finally, we note that the present calculations assume full disorder between Cu and Fe, and also that both Fe and Cu remain in the Fe plane and do not occupy other sites, such as the excess Fe site in the interstitial. It will be useful to test the extent to which these assumptions hold for the real material, for example by using diffraction to refine the occupancy of the interstitial site.

Acknowledgments

The authors are much indebted to Roser Valenti and Jürgen Kübler for helpful discussions. The financial support by the SFB/TRR49 is gratefully acknowledged. Work at Oak Ridge National Laboratory was supported by the Department of Energy, Division of Materials Sciences and Engineering.

---

[*] Electronic address: chadov@uni-mainz.de

[1] Y. Kamihara, T. Watanabe, M. Hirano, and H. Hosono, J.

Amer. Chem. Soc. **130**, 3296 (2008).

[2] S. E. Sebastian, J. Gillett, N. Harrison, P. H. C. Lau, D. J. Singh, C. H. Mielke, and G. G. Lonzarich, J. Phys. Condens. Matter **20**, 422203 (2008).

[3] D. H. Lu, M. Yi, S. K. Mo, A. S. Erickson, J. Analytis, J. H. Chu, D. J. Singh, Z. Hussain, T. H. Geballe, I. R. Fisher, et al., Nature (London) **455**, 81 (2008).

[4] W. L. Yang, A. P. Sorini, C. C. Chen, B. Moritz, W. S. Lee, F. Vernay, P. Olalde-Velasco, J. D. Denlinger, B. Delley, J. H. Chu, et al., Phys. Rev. B **80**, 014508 (2009).

[5] F.-C. Hsu, J.-Y. Luo, K.-W. Yeh, T.-K. Chen, T.-W. Huang, P. M. Wu, Y.-C. Lee, Y.-L. Huang, Y.-Y. Chu, D.-C. Yan, et al., Proc. Nat. Acad. Sci. (USA) **105**, 14262 (2008).

[6] Y. Mizuguchi, F. Tomioka, S. Tsuda, T. Yamaguchi, and Y. Takano, Appl. Physics Lett. **93**, 152505 (2008).

[7] S. Medvedev, T. M. McQueen, I. Troyan, T. Palasyuk, M. Eremets, R. J. Cava, S. Naghavi, F. Casper, V. Ksenofontov, G. Wortmann, et al., Nature Materials **8**, 630 (2009).

[8] S. Margadonna, Y. Takabayashi, Y. Ohishi, Y. Mizuguchi, Y. Takano, T. Kagayama, T. Nakagawa, M. Takata, and K. Passides, Phys. Rev. B **80**, 064506 (2009).

[9] G. Garbarino, A. Sow, P. Lejay, A. Sulpice, P. Toulemonde, W. Crichton, M. Mezouar, and M. Núnez-Regueiro, Europhys. Lett. **86**, 27001 (2009).

[10] T. Imai, K. Ahilan, F. L. Ning, T. M. McQueen, and R. J. Cava, Phys. Rev. Letters **102**, 17705 (2009).

[11] I. I. Mazin, M. D. Johannes, L. Boeri, K. Koepernik, and D. J. Singh, Phys. Rev. B **78**, 085104 (2008).

[12] D. J. Singh, Physica C **469**, 418 (2009).

[13] L. Boeri, O. V. Dolgov, and A. A. Golubov, Phys. Rev. Letters **101**, 026403 (2008).

[14] Z. P. Yin, S. Lebegue, M. J. Han, B. P. Neal, S. Y. Savrasov, and W. E. Pickett, Phys. Rev. Letters **101**, 047001 (2008).

[15] D. J. Singh and M. H. Du, Phys. Rev. Lett. **100**, 237003 (2008).

[16] I. I. Mazin, D. J. Singh, M. D. Johannes, and M. H. Du, Phys. Rev. Lett. **101**, 057003 (2008).

[17] A. Subedi, L. Zhang, D. J. Singh, and M. H. Du, Phys. Rev. B **78**, 134514 (2008).

[18] Z. Liu, A. Fang, F. Huang, and M. Jiang, arXiv:0808.1784v1 (2008).

[19] T. M. McQueen, Q. Huang, V. Ksenofontov, C. Felser, Q. Xu, H. Zandbergen, Y. S. Hor, J. Allred, A. J. Williams, D. Qu, et al., Phys. Rev. B **79**, 014522 (2009).

[20] A. J. Williams, T. M. McQueen, and R. J. Cava, Solid State Commun. **149**, 1507 (2009).

[21] T. M. McQueen, A. J. Williams, P. W. Stephens, J. Tao, Y. Zhu, V. Ksenofontov, F. Casper, C. Felser, and R. J. Cava, Phys. Rev. Lett. **103**, 057002 (2009).

[22] C. de la Cruz, Q. Huang, J. W. Lynn, J. Li, W. R. II, J. L. Zarestky, H. A. Mook, G. F. Chen, J. L. Luo, N. L. Wang, et al., Nature (London) **453**, 899 (2008).

[23] G. F. Chen, Z. Li, D. Wu, G. Li, W. Z. Hu, J. Dong, P. Zheng, J. L. Luo, and N. L. Wang, Phys. Rev. Lett. **100**, 247002 (2008).

[24] F. Ma and Z. Lu, Phys. Rev. B **78**, 033111 (2008).

[25] J. Dai, Q. Si, J.-X. Zhu, and E. Abrahams, Proc. Nat. Acad. Sci. USA **106**, 4118 (2009).

[26] K.-W. Lee, V. Pardo, and W. E. Pickett, Phys. Rev. B **78**, 174502 (2008).

[27] M. J. Han and S. Y. Savrasov, Phys. Rev. Letters **103**, 067001 (2009).

[28] A. J. Williams, T. M. McQueen, V. Ksenofontov, C. Felser, and R. J. Cava, J. Phys.: Condens. Matter **21**, 305701 (2009).

[29] J. P. Perdew, K. Burke, and M. Ernzerhof, Phys. Rev. Lett. **77**, 3865 (1996).

[30] G. Kresse and D. Joubert, Phys. Rev. B **59**, 1758 (1999).

[31] Y. Li, X. Lin, Q. Tao, C. Wang, T. Zhou, L. Li, Q. Wang, M. He, G. Cao, and Z. Xu, New J. Phys. **11**, 053008 (2009).

[32] D. J. Singh and L. Nordstrom, *Planewaves, Pseudopotentials and the LAPW Method, 2nd Ed.* (Springer Verlag, 2006).

[33] E. Sjostedt, L. Nordstrom, and D. J. Singh, Solid State Commun. **114**, 15 (2000).

[34] P. Blaha, K. Schwarz, G. Madsen, D. Kvasnicka, and J. Luitz, WIEN2k, An Augmented Plane Wave + Local Orbitals Program for Calculating Crystal Properties (K. Schwarz, Tech. Univ. Wien, Austria) (2001).

[35] V. Milman, Acta Cryst. **B58**, 437 (2002).

[36] A. S. Sefat, R. Jin, M. A. McGuire, B. C. Sales, D. J. Singh, and D. Mandrus, Phys. Rev. Lett. **101**, 117004 (2008).

[37] B. Gyorffy, Phys. Rev. B **5**, 2382 (1972).

[38] G. M. Stocks and H. Winter, *The electronic structure of complex systems* (Plenum Press, New York, 1984), p. 463.

[39] W. H. Butler, Phys. Rev. B **31**, 3260 (1985).

[40] P. A. Lee and T. V. Ramakrishnan, Rev. Mod. Phys. **57**, 287 (1985).

[41] Another interesting possibility is that moments could form on the neighboring Fe but that these could form singlets where the four Fe atoms around the Cu could have cancelling moments due to antiferromagnetic interactions between them. Recalling that the four Fe atoms around a Cu substitutional are second neighbors on the Fe square lattice, the case where the Fe moments are aligned would correspond locally to the checkerboard (nearest neighbor antiferromagnetic) order, while the antiferromagnetic state with cancelling Fe moments would correspond locally to the SDW pattern.

[42] Y. A. Dorofeev, A. Z. Men'shikov, and V. G. Pleshchev, Physics of the Solid State **36**, 1329 (1994).

[43] J. C. Woolley, A. M. Lamarche, G. Lamarche, R. Brun del Re, M. Quintero, F. Gonzales-Jimenez, I. P. Swainson, and T. M. Holden, J. Magn. Magn. Mater. **164**, 154 (1996).

[44] S. Mankovskyy and H. Ebert, Phys. Rev. B **74**, 54414 (2006).

[45] F. Baudelet, S. Odin, C. Giorgetti, E. Dartyge, J. P. Itie, A. Polian, S. Pizzini, A. Fontaine, and J. P. Kappler, J. Phys. (Paris) **7**, C2 441 (1997).

[46] V. Crisan, P. Entel, H. Ebert, A. Akai, D. D. Johnson, and J. B. Staunton, Phys. Rev. B **66**, 014416 (2002).

[47] N. M. Rosengaard and B. Johansson, Phys. Rev. B **55**, 14975 (1997).

[48] A. J. Pindor, J. Staunton, G. M. Stocks, and H. Winter, J. Phys. F: Met. Phys. **13**, 979 (1983).

[49] B. L. Gyorffy, A. J. Pindor, J. Staunton, G. M. Stocks, and H. Winter, J. Phys. F: Met. Phys. **15**, 1337 (1985).

[50] A. V. Ruban, S. Khmelevskyi, P. Mohn, and B. Johansson, Phys. Rev. B **75**, 054402 (2007).

[51] H. Ebert and M. Battocletti, Solid State Commun. **98**, 785 (1996).

[52] S. H. Vosko, L. Wilk, and M. Nusair, Can. J. Phys. **58**, 1200 (1980).

[53] A. I. Liechtenstein, M. I. Katsnelson, V. P. Antropov, and V. A. Gubanov, J. Magn. Magn. Materials **67**, 65 (1987).

[54] Y.-F. Li, L.-F. Zhu, S.-D. Guo, Y.-C. Xu, and B.-G. Liu, J. Phys.: Condens. Matter **21**, 115701 (2009).

[55] F. Ma, W. Ji, J. Hu, Z.-Y. Lu, and T. Xiang, Phys. Rev. Letters **102**, 177003 (2009).